Specific Ion Influences on Self-Association of Pyruvate Dehydrogenase Kinase Isoform 2 (PDHK2), Binding of PDHK2 to the L2 Lipoyl Domain, and Effects of the Lipoyl Group-Binding Site Inhibitor, Nov3r†

Yasuaki Hiromasa, Xiaohua Yan, and Thomas E. Roche*

Department of Biochemistry, Kansas State University, Manhattan, Kansas 66506

Received July 25, 2007; Revised Manuscript Received November 16, 2007

ABSTRACT: Association of the PDHK2 and GST-L2 (glutathione-*S*-transferase fused to the inner lipoyl domain (L2) of dihydrolipoyl acetyltransferase (E2)) dimers was enhanced by K^+ with higher affinity K^+ binding than occurs at the PDHK2 active site. Supporting a distinct K^+ binding site, the NH_4^+ ion did not effectively replace K^+ in aiding GST-L2 binding. With 50 mM K^+, P_i enhanced interference by ADP, ATP, or pyruvate of PDHK2 binding to GST-L2. The inclusion of P_i with ADP or ATP plus pyruvate greatly hindered PDHK2 binding to GST-L2 and promoted PDHK2 forming a tetramer. Reciprocally, GST-L2 interference with ATP/ADP binding also required elevated K^+ and was increased by P_i. Potent inhibition by Nov3r of E2-activated PDHK2 activity (IC50 of ∼7.8 nM) required elevated K^+ and P_i. Nov3r only modestly inhibited the low activity of PDHK2 without E2. By binding at the lipoyl group binding site, Nov3r prevented PDHK2 binding to E2 and GST-L2. Nov3r interfered with high-affinity binding of ADP and pyruvate via a P_i-dependent mechanism. Thus, GST-L2 binding to PDHK2 is supported by K^+ binding at a site distinct from the active site. P_i makes major contributions to ligands interfering with PDHK2 binding to GST-L2, the conversion of PDHK2 dimer to a tetramer, and Nov3r (an acetyllipoate analog) interfering with binding of ADP and pyruvate. P_i is suggested to facilitate transmission within PDHK2 of the stimulatory signal of acetylation from the distal lipoyl-group binding site to the active site.

When carbohydrate stores are reduced, mammalian pyruvate dehydrogenase complex (PDC)[1] activity is downregulated to limit the oxidative utilization of glucose in most nonneural tissues (*1*−*5*). When there is surplus carbohydrate or urgent energy requirements, upregulation of PDC activity allows carbohydrate to be oxidatively used and is needed for the conversion of surfeit dietary carbohydrate to fatty acids. Control of the downregulation and upregulation of PDC activity primarily occurs via effector control of the phosphorylation state of the PDC. Phosphorylation with inactivation of the pyruvate dehydrogenase (E1) component is catalyzed by pyruvate dehydrogenase kinase (PDHK) and dephosphorylation with reactivation by pyruvate dehydrogenase phosphatase (*6*).

PDC activity is restricted in many tissues when fatty acids and/or ketone bodies are used as the primary fuel sources, resulting in elevated levels of intramitochondrial acetyl-CoA and NADH, which enhances PDHK activity (*1*−*5*, *7*−*10*). To increase PDHK activity, these products are first used to reductively acetylate lipoyl domains of dihydrolipoyl acetyltransferase oligomer (E2) component of PDC via the reverse of the dihydrolipoyl dehydrogenase (E3) and E2 reactions. PDHK activity is then stimulated by interaction with acetylated-lipoyl domains (*3*, *4*, *11*−*15*). E2 has two lipoyl domains (L1 and L2) (*3*, *16*) and the E3 binding protein (E3BP) has one lipoyl domain (*3*, *17*). Particularly important for PDHK2 stimulation is the reductive acetylation of the inner L2 domain that most effectively binds PDHK2 (*3*, *4*, *15*, *18*−*20*). On a per lipoyl domain basis, PDHK2 binding is appreciably stronger to the bifunctional GST-L2 dimer (or E2 60mer) than to the L2 monomer (*21*). Lipoyl group reduction and to a greater extent successive acetylation enhance PDHK2 binding to GST-L2 and E2 (*20*, *21*). In the opposite direction, ADP and pyruvate inhibit PDHK2 activity (*19*, *22*) and reduce the binding of PDHK2 to L2 (*23*). The companion paper[2] shows that K^+ and P_i greatly increase binding by ADP and pyruvate; here we show that these ions also play critical roles in ADP and pyruvate interfering with binding of PDHK2 to the L2 domain. However, we additionally find evidence that K^+ enhances PDHK2 binding to GST-L2 by binding at a site that differs from the site promoting ADP/ATP binding.

† This work was supported by National Institutes of Health Grant DK18320, the American Heart Association, AstraZeneca, and the Agricultural Experiment Station (Contribution 08-31-J).

* To whom correspondence should be addressed. Phone: 785-532-6116. Fax: 785-532-7278. E-mail: bchter@ksu.edu.

[1] Abbreviations used: PDC, pyruvate dehydrogenase complex; E1, pyruvate dehydrogenase component; E2, dihydrolipoyl acetyltransferase component; L1 domain, NH_2-lipoyl domain of E2; L2 domain, interior lipoyl domain of E2; E3, dihydrolipoyl dehydrogenase; E3BP, E3-binding protein; PDHK, pyruvate dehydrogenase kinase; GST, glutathione-*S*-transferase; GST-L2, GST-L2 fusion protein dimer; DCA, dichloroacetate; AUC, analytical ultracentrifugation.

[2] Companion paper: Hiromasa, Y., and Roche, T. E. (2008) Critical Role of Specific Ions for Ligand-Induced Changes Regulating Pyruvate Dehydrogenase Kinase Isoform 2, *Biochemistry 47,* 2298−2311.

10.1021/bi7014772 CCC: $40.75
Published on Web 01/26/2008

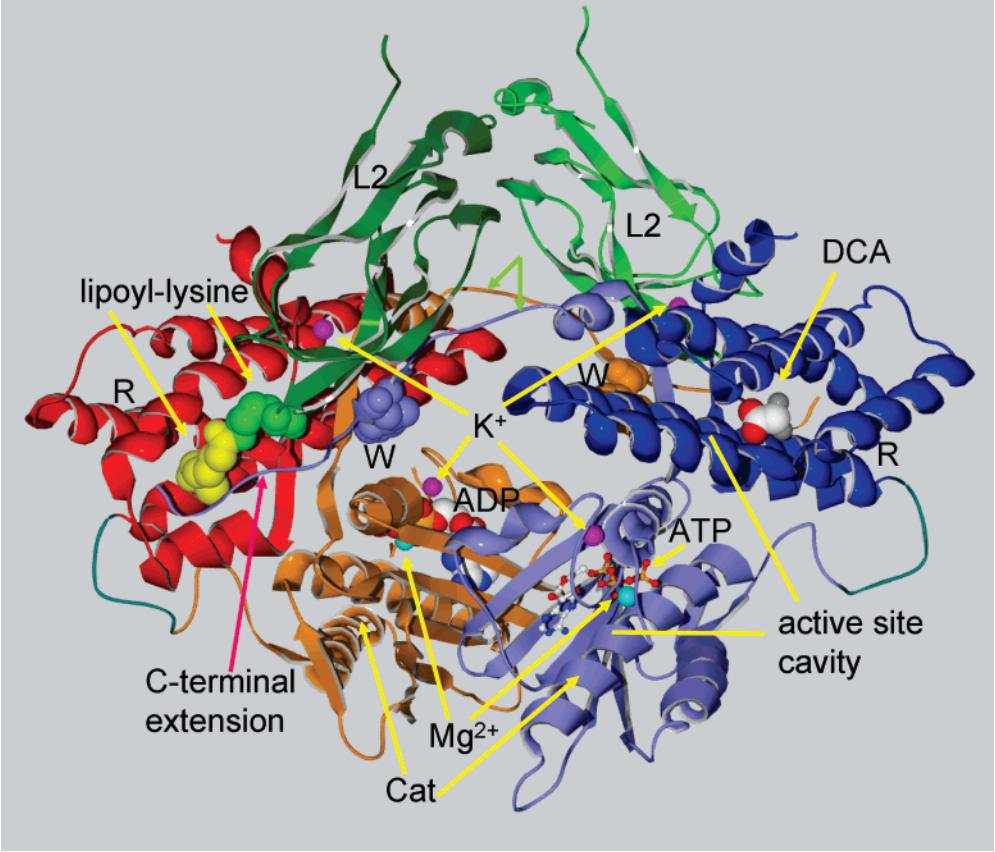

FIGURE 1: PDHK•L2 dimer structure. The PDHK3•L2•ATP (*25*; 1Y8O), PDHK3•L2•ADP (*25*; 1Y8P), and PDHK2•ADP•DCA (*26*; 2bu8) structures were aligned using DeepView magic align and then specific structure exhibited from different pdb with proteins as ribbon structures. The close alignment of the backbone 3-D structures of PDK2 and PDK3 were previously exhibited (Supporting Information, *ref 26*). The regulatory (R) and catalytic (Cat) domains of PDHK3 are shown in red and orange in the left subunit and blue and violet in the right subunit. At the top, one L2 domain (left) is shown in dark green with lipoyl-lysine (space filled) and the other L2 domain (right) in lighter green without the lipoyl lysine for clarity. Near upper center of trough region, the cross arms are marked with a bright green double arrow. Space-filled Trp (W) are shown at the end of the cross arms (Trp381 of PDHK3, which aligns with Trp383 of PDHK2; residue numbering and alignment of mature PDHK isoforms are as shown in Supporting Information (*ref 26*). The C-terminal extension beyond W381 for the cross arm comes from the Cat subunit on right is labeled on the left; parts of the equivalent structure (orange) can be seen behind the R domain on right. The location of the DCA in the right subunit is based on DCA binding site in PDHK2 (*26*). The figure locates the Mg^{2+} (dark cyan in each subunit) that chelate to an oxygen of β-phosphate of ATP and ADP and an oxygen of the γ-phosphate of ATP at the active site. The K^+ ions are shown in magenta. These include K^+ that chelate to an oxygen of α-phosphate of ATP (stick structure, right subunit) and to ADP (space filled, left subunit) and K^+ that are bound on the trough side of R domain in each subunit.

PDHK subunits have a catalytic (Cat) domain and a regulatory (R) domain (*24*−*27*). ATP/ADP are bound by the Cat domain (*24*); pyruvate/DCA (*26*) and the lipoyl group of L2 (*25*) are bound by the R domain (Figure 1). Catalytic cavities are formed between these domains at opposite ends of the PDHK dimer. The dimer structure is formed by association of the Cat domains. A secondary interaction between subunits involves cross arms produced by the near C-terminal ends of the Cat domains spanning a trough region that has the interacting Cat domains as a base and R domains as the upper walls (*25*−*27*). At the end of the cross arm, a tryptophan residue (Trp383, PDHK2; Trp381, PDHK3, labeled with W in Figure 1) lodges between the interface of the R and Cat domain of the other subunit. The PDHK3 isoform, which binds L2 domain tighter than PDHK2, has been crystallized with two L2 domains bound (Figure 1) (*25*, *27*). The L2 domain interacts with the intersubunit cross arms and with C-terminal extensions of these cross arms that pass under the lipoyl domain and then alongside the lipoyl group binding site of the other subunit (Figure 1). The importance of equivalent (*25*) versus nonequivalent (*27*) binding of L2 by PDHK3 needs to be established.

In potassium phosphate buffer, ADP and pyruvate caused a marked reduction in binding of PDHK2 to the GST-L2 (*23*). Furthermore, these ligands caused the PDHK2 dimer to associate as a tetramer (*23*). Both changes act to greatly hinder PDHK2 activity, helping to explain the potent inhibition by the combination of these effectors. Here we use these approaches to establish critical roles of K^+ and P_i in effector modulation of PDHK2 dimer binding to GST-L2 and the conversion of the PDHK2 dimer to a tetramer. Evidence is provided for low K^+ levels aiding L2 associating with the L2 domain by K^+ binding at a site that is distinct from the site at which K^+ or NH_4^+ assist ATP and ADP binding[2]. Because it is almost certainly the case and for ease of referencing the different K^+ roles/sites, we will assume here that the latter constitutes K^+ being bound at the active site that includes direct chelation to an oxygen of the α-phosphate group of ATP and ADP (*25*, *26*). Interestingly, a bound K^+ ion is found in the PDHK3•L2 structure (*25*) located in the R domain adjacent to the L2 binding site (Figure 1). We show that P_i is required for strong effector interference with L2 binding and for tetramer formation.

Related trifluoro-2-hydroxy-2-methylpropionate compounds (Nov3r, AZD7545, AZ12, compound K) are potent inhibitors of PDHK activity (*4*, *28*−*31*). PDC activity is markedly reduced in diabetic animals due to high PDHK activity (*1*−*5*, *32*−*35*); the very low PDC activity hinders use of glucose as an energy source. AZD7545 and compound K have been used to inhibit PDHK activity and increase PDC in Zucker fa/fa obese rats (a model for insulin resistant diabetes) (*36*, *37*). Treatment of obsese Zucker rats with compound K reduced the aberrantly high blood glucose to extents similar to the commonly used drug, rosiglitazone (*37*). PDHK2 crystal structures have been obtained with Nov3r and AZ12 bound at the lipoyl binding site (*26*) (see Figure 1, the companion paper[2]). Based on comparative modeling of K^+ binding at the active site in PDHK2 crystal structures, the binding of Nov3r appeared to introduce a conformational change in PDHK2 that hinders K^+ binding by the PDHK2 active site containing a bound ATP (*26*). Such a change would be expected to weaken ATP and ADP binding and speed up PDHK2 catalysis in which ADP dissociation appears to be rate limiting (*20*).

Here, we demonstrate that Nov3r prevents PDHK2 binding to L2 and dissect the effects of Nov3r binding at the lipoyl group binding site on PDHK2 binding of other ligands. Again, we establish critical roles of ions for high affinity binding of Nov3r, for Nov3r interfering with binding of L2, and for Nov3r altering the binding of other ligands. In addition to K^+, P_i is found to play a critical role in Nov3r, bound at the lipoyl binding site, influencing ligand binding at other sites, including weakening ADP and pyruvate binding. Our studies establish key linkage roles of K^+ and P_i in the transmission of regulatory effects that reduce and enhance PDHK2 activity.

EXPERIMENTAL PROCEDURES

Materials. Along with those indicated in the companion paper (*19*, *22*, *38*), the additional human PDC components purified were E2•E3BP (*Supporting Information*, (*38*)), GST-L2 (*39*), and E3 (*40*). PDHK2 was prepared in 50 mM potassium phosphate buffer, pH 7.5 or 20 mM Hepes-Tris buffer, pH 7.5 (buffer A) free of K^+ and P_i as described (*23*).[2] Nov3r (*28*) was provided as the pure stereoisomer by Roger J. Butlin at AstraZeneca, Macclesfield, Great Britain.

Fluorescence Quenching. To evaluate ligand binding, Trp-fluorescence quenching was carried out and analyzed as previously described (*23*).[2] Unless otherwise indicated, studies were conducted with 2 mM free Mg^{2+} initially available prior to addition of ligands. Nov3r is maximally added at 10 μM in fluorescence quenching studies; this level of Nov3r has an absorbance <0.01 at 295 nm and no absorbance above 310 nm. The conditions for studies using fluorescence quenching with high levels of PDHK2 dimer (4.3 μM) with and without 12.8 μM GST-L2 dimer are described in the Supporting Information section.

Analytical Ultracentrifuge (AUC) Experiments. Sedimentation velocity experiments were conducted as previously described (*20*, *21*, *23*, *38*, *41*) using an Optima XL-I ultracentrifuge using the An-60 Ti rotor at 20 °C in buffer A with 5 mM dithiothreitol, 0.5 mM EDTA and the indicated ligands. Sedimentation was monitored at 280 nm using double sector cells with a final loading of 400 μL per cell. Sedimentation was at 49,000 rpm with scans made at 5 min intervals. Ligand-induced changes in the interaction of PDHK2 with GST-L2 and ligand-induced self-association of PDHK2 were evaluated by sedimentation velocity studies using the concentrations of components indicated in figure legends.

Sedimentation data were analyzed using DCDT+ software version 1.16 and sedimentation coefficients were calculated by using $g(s^*)$ fitting function in DCDT+ software (*42*, *43*). Buffer density and viscosity were calculated by Sednterp version 1.08 (www.jphilo.mailway.com) or were measured as previously described (*38*). The partial specific volumes of proteins (*21*, *38*) were calculated from their amino acid composition using Sednterp (0.734 for human PDHK2 at 20 °C). The apparent sedimentation coefficient distribution function $g(s^*)$ versus s^* provides useful boundary shape for evaluating associating systems (*42*−*45*). With the different concentrations of ions (K^+, NH_4^+, or Na^+ and counterions), the sedimentation velocity profiles were converted for comparison to a low salt condition using the changes in the sedimentation of GST-L2, PDHK2, and E3 alone as standards for adjusting the effects of changes in density and viscosity. Support for this approach was obtained using different KCl levels in potassium phosphate buffer. Adjustments based on the known changes in density and viscosity gave the same correction of $g(s^*)$ versus s^* profiles within experimental error for E3, fitting little if any change in the frictional coefficient of E3. The change with different ligands in the equilibrium binding of PDHK2 to GST-L2 was assessed by simulating the $g(s^*)$ profiles using the SedAnal program (*43*−*45*) and the $A + B = C$ model, as previously described (*23*, *41*). The self-association of PDHK2 dimer to a tetramer was analyzed by monomer−dimer equilibrium model using the SEDPHAT 2.02 program (*46*, *47*). All of the softwares used in these analyses are available from the RASMB site (www.asmb.bbri.org/RASMB/rasmb.html).

PDHK2 Activity Assays. The inhibition of PDHK2 activity by Nov3r and related inhibitors was first evaluated with buffer systems containing 100 mM K^+ and (Cl^-) or minimal (<15 mM) K^+ ion and measuring the ^{32}P-incorporation at 30 °C using just E1 (12 μg) or E2-E1 (7 μg E1, 10 μg E2) as substrate in 25 μL final volume (*14*, *19*, *20*, *22*). The standard buffer contained 40 mM Mops adjusted to pH 7.4 with Tris and 13 mM K_xPO_4 (pH 7.4) with 2 mM dithiothreitol, 2 mM $MgCl_2$, 0.1 mM EDTA, and 0.1% Pluronics F68. Additionally 40 mM K^+ (prepared with KOH adjusted to pH 7.4 with Hepes) and 60 mM KCl were included for high salt buffer. The activity of 0.15 μg PDHK2 (E2•E1 substrate) or 0.3 μg E1 (E1 as substrate) was initiated by addition of [γ-^{32}P]ATP to 100 μM and terminated after 60 s or 120 s, respectively. Even at 100 μM Nov3r comes out of solution with time (decreasing absorbance observed) unless it is maintained with at least 5% DMSO. A 50 μM Nov3r concentrate was prepared in 10% DMSO; kinase reaction mixtures did not contain >0.5% DMSO. Assays were conducted at least in duplicate; average values with standard deviations are shown.

To estimate the IC50 of Nov3r, the following PDC inactivation assay was used so that PDHK2 concentration could be reduced to 1.2 nM. The inactivation of PDC (0.9 μg E1, 1.0 μg E2•E3BP, 0.4 μg E3) by 0.011 μg PDHK2 was initiated in 100 μL final volume of 50 mM Mops-K

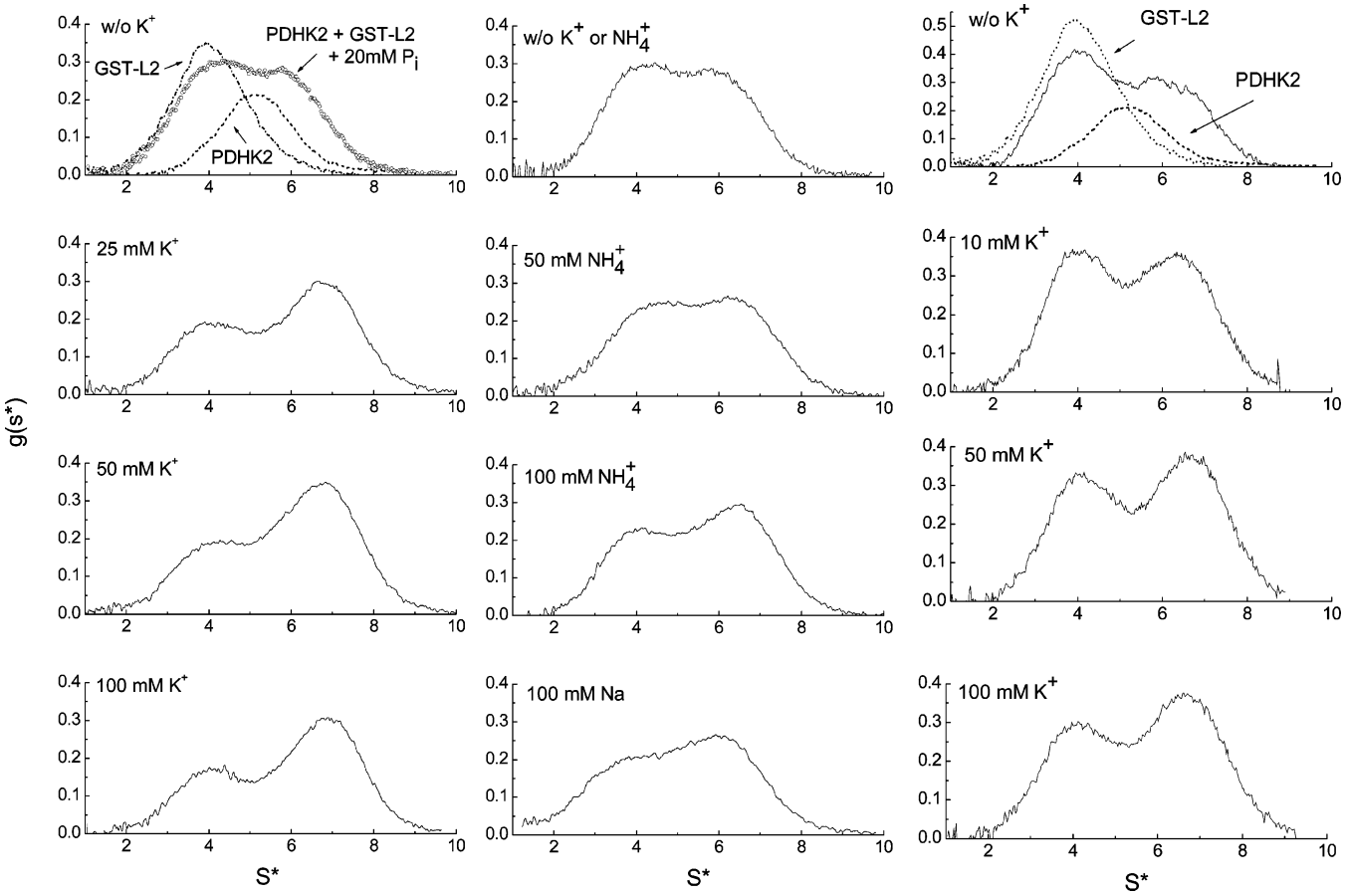

FIGURE 2: Cation effects and concentration dependence for binding of PDHK2 to GST-L2 in the absence and presence of ATP. All buffers contained 5 mM dithiothreitol and 0.5 mM EDTA. The series in the left column (bottom three panels) show the change in $g(s^*)$ profiles for sedimentation velocity studies conducted with 4.3 μM PDHK2 plus 5.7 μM GST-L2 (*21*, *23*) with indicated K^+ levels; control with no K^+ (or NH_4^+) is shown in top panel in center column. The top panel in the left column shows the $g(s^*)$ profiles for the same levels of PDHK2 and GST-L2, alone, and for the combination with 20 mM P_i in the absence of K^+ (or NH_4^+). The middle column shows the effects of 50 and 100 mM NH_4^+ and 100 mM Na^+ on the sedimentation velocity patterns with the same level of protein components. The right column shows a series of $g(s^*)$ profiles in which the level of K^+ was varied in the presence of 100 μM ATP with 4.3 μM PDHK2 with the GST-L2 level increased to 8.5 μM. The $g(s^*)$ profiles are corrected for changes in viscosity and density using the approach described under Experimental Procedures. Sedimentation velocity studies were conducted at additional levels of ions as indicated in the text.

(pH 7.3), 50 mM KCl, 1 mM EDTA, 2 mM dithiothreitol, 2 mM $MgCl_2$, 0.5 mM EDTA, 0.1% Pluronics F68, and 0.2 mg/mL BSA by addition of ATP to100 μM. At 120 and 240 s, 40 μL samples were pulled and added to10 μL containing 50 mM glucose and 1 μg hexokinase to stop PDHK2 reaction by converting ATP to ADP; this mixture was maintained on ice until PDC activity was measured. PDC activity was measured in duplicate by adding 20 μL samples to 200 μL final volume in cuvettes pre-equilibrated at 30 °C for 3−5 min that additionally contained 1 μg E2·E3BP, 1.25 μg E3 and 50 mM Mops-K, pH 7.4, 2.5 mM NAD^+, 0.3 mM thiamine pyrophosphate, 0.25 mM CoA, 2.5 mM cysteine, 2 mM $MgCl_2$, and 0.1 mg/mL BSA. After incubation for 60 s, four assays were initiated simultaneously by addition of pyruvate to 2.0 mM with mixing; NADH production was measured at 340 nm for 5−10 min using a Beckman DU670 spectrophotometer. Control PDC activity was measured in duplicate at the beginning and end of the experiments by substituting water for ATP. These four measures of control PDC activity at the beginning and the end of assay series established that the control PDC activity remained constant within experimental error; inclusion of Nov3r even at levels above those tested had no effect on PDC activity. No more than 40% reduction of PDC activity was used in measuring PDHK2-catalyzed inactivation of PDC; within this range, the reduction of PDC activity at 4 min was generally twice that at 2 min. The standard deviation from the average was less than ±2% for control activity and generally below ± 4% for estimates of the reduction in PDC activity. A few assays were conducted just using 0.9 μg E1 as a substrate in the absence of E2 using reaction times of 10 and 25 min; after removal of ATP by hexokinase reaction, 1.0 μg E2•E3BP and 0.4 μg E3 were added (volume 55 μL) and the reconstituted PDC activity subsequently was measured on 22 μL as described above. Other properties of these assays are described under Results.

RESULTS

Effects of Ions on Binding of PDHK2 to the L2 Domain. The co-localization of PDHK and the E1 substrate on E2 oligomer and movement of PDHK between lipoyl domains greatly enhances kinase activity (*3*, *4*, *14*, *19*−*21*, *48*). PDHK2 preferentially binds to the L2 domain (*19*, *21*). In potassium phosphate buffer, there was a strong correlation between conditions that led to ligand-induced quenching of PDHK2 fluorescence and those that diminished binding of

the dimeric PDHK2 to dimeric GST-L2 containing a reduced lipoyl groups (*23*); a condition that strengthens binding by PDHK2 (*21*) and was used in the following studies. In the absence of K^+ or NH_4^+, some binding of 4.3 μM PDHK2 to 5.7 μM GST-L2 was observed (Figure 2, top panel, center column) and this level of binding was not significantly changed by 20 mM P_i (Figure 2, top panel column 1) Simulation of the sedimentation profiles (*21*) indicated ~45% of PDHK2 was associated with GST-L2 in the absence of K^+, which fits a 1:1 complex with a K_d of 4−5 μM. Inclusion of 25 mM K^+ ion enhanced binding (~66% PDHK2 bound); further increases to 50 or 100 mM K^+ supported formation of only slightly more complex (Figure 2, left column series). With 150 mM K^+, there was no further increase in binding (data not shown). The fractional binding of 0.69−0.75 estimated at these higher levels of K^+ corresponds to a K_d of ~1 μM, which is similar to results obtained in 50 mM potassium phosphate buffer (*21*, *23*).

Higher levels of NH_4^+ than K^+ were needed to give any enhancement in binding with some increase in complex formation as the level of NH_4^+ was increased from 25 (data not shown) to 50 and then 100 mM (Figure 2, middle column). 100 mM Na^+ also supported some increase in complex formation (Figure 2, bottom panel, middle column) though much less effectively than 25 mM K^+ but nearly as well as 100 mM NH_4^+. Although these results demonstrate an enhancement in PDHK2 binding to GST-L2 by the monovalent cation, the results diverge from the monovalent cation requirements for ATP/ADP-induced Trp-fluorescence quenching[2]. The concentration dependence for near saturation of the K^+ in supporting PDHK2•GST-L2 complex formation is below the K_d estimated for K^+ binding to free PDHK2 (Table 4, companion paper[2]). Higher rather than lower NH_4^+ levels are required, and even then the NH_4^+ ion is much less effective than K^+ in supporting lipoyl domain binding. Thus, these results raise the question whether the monovalent ions are binding at a different site or whether GST-L2 binding alters monovalent cation binding at the same site, presumably the active site. The latter would require strengthening of K^+ binding while weakening NH_4^+ binding. Enhanced K^+ binding at the active site would be expected to enhance ADP and ATP binding[2] but the opposite was found (below). The capacity of 100 mM Na^+ to support some enhancement in binding to GST-L2 also supports a separate site.

Impact of K^+ and NH_4^+ on PDHK2·GST-L2 Complex Formation in the Presence of ATP. With 100 μM ATP included, the concentration dependence for K^+ and NH_4^+ enhancing binding of 4.3 μM PDHK2 to 8.5 μM GST-L2 was evaluated. ATP decreases PDK2 binding to GST-L2 with 50 mM K^+ (Figure 3, below). There was a substantial increase in complex formation as K^+ was introduced and increased (Figure 2, third column) but only a small increase above 50 mM K^+. With increasing K^+ (0, 10, 20, 50, and 100 mM), the estimated S_{wav} also increased (5.01, 5.26, 5.47, 5.53, and 5.61 S; errors ± 0.07 S). Under these conditions but with saturating K^+, the maximal S_{wav} is projected to be 5.72 S. The half-maximal increase in S_{wav} is then attained at <20 mM K^+. In the absence of ATP, the half-maximal increase in S_{wav} was reached with <7 mM K^+. The increase in K^+ dependence contrasts with the effects of ATP in greatly enhancing K^+ binding at the active site as measured by Trp-fluorescence quenching[2]. With the NH_4^+ ion varied with 100 μM ATP, the increases in complex formation with increasing NH_4^+ ion were much smaller (S_{wav} only increased from 5.01 S to 5.04, 5.13, and 5.19 S with 10, 50, and 100 mM NH_4^+). If the binding affinity of NH_4^+ is the only limitation, for NH_4^+ being as effective as K^+ in aiding PDHK2 binding to GST-L2, then a K_d >150 mM NH_4^+ would be required for NH_4^+ supporting full GST-L2 binding under these conditions. That is >500 fold higher than $L_{0.5}$ for NH_4^+ binding at the active site in the presence of 100 μM ATP. Again, these results are most easily explained by K^+ binding at a separate site from the active site being weakened by ATP and by very weak NH_4^+ ion binding at that alternative site that is further weakened by ATP binding at the active site. The possibility that only changes in monovalent cation binding at the active site of PDHK2 produce the above results is very unlikely.

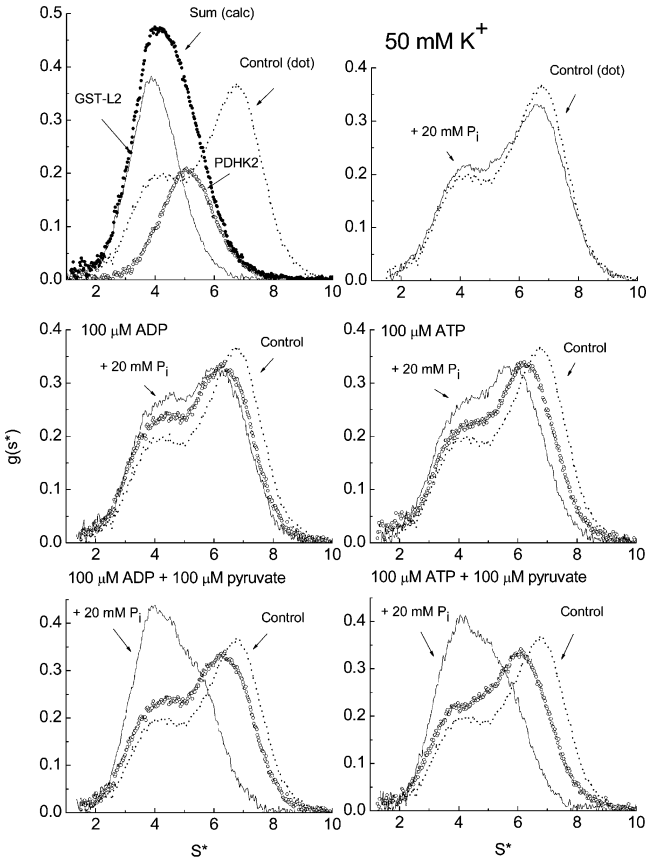

FIGURE 3: Change in binding of PDHK2 with GST-L2 due to addition of ligands. The changes in sedimentation velocity $g(s^*)$ profiles of 4.3 μM PDHK2 with 8.5 μM GST-L2 were evaluated with 50 mM K^+, 5 mM dithiothreitol, and 0.5 mM EDTA included in all studies along with the indicated ligands. The left panel at the top shows the sum of profiles for PDHK2 plus GST-L2 alone as an indicator of profile expected with binding prevented. The top panels show the effects of 20 mM P_i; the middle panels show the effects of 100 μM ATP (left) or 100 μM ADP (right) with and without 20 mM P_i; and the bottom panels include 100 μM pyruvate along with the conditions used in the middle panels. Sedimentation velocity patterns were corrected for changes in density and viscosity as described under Experimental Procedures.

We were unable to evaluate whether the concentration dependencies of the NH_4^+ ion in supporting quenching of Trp fluorescence by ATP or ADP were altered by GST-L2 binding because fluorescence could not be evaluated at the very high levels of GST-L2 and PDHK2 that are required

to have predominantly PDHK2•GST-L2 complex formed in the absence of added ions.

Critical Role of P_i in Support of Ligands interfering with PDHK2 Binding to GST-L2. Prior studies (*23*) in potassium phosphate buffer demonstrated that ADP or ATP plus pyruvate greatly reduced PDHK2 binding to GST-L2. We evaluated the effects of ligands (100 μM ATP or ADP alone or with 100 μM pyruvate) in reducing PDHK2•GST-L2 complex formation with or without 20 mM P_i in the presence of 50 mM K^+ (Figure 3) or 50 mM NH_4^+ (Figure 2S, Supporting Information). P_i had a very small effect by itself as did ATP or ADP in the absence of P_i. With 50 mM K^+, P_i enhanced interference with binding PDHK2 to GST-L2 with ATP or ADP (middle panels Figure 3). When P_i was included along with pyruvate and ATP or ADP, complex formation was nearly eliminated (bottom panels, Figure 3). Thus, 20 mM P_i works synergistically with pyruvate plus ADP or ATP in blocking formation of the PDHK2•GST-L2 complex just as P_i acts with these ligands to maximize fluorescence quenching. At higher levels of components, some complex formation could be demonstrated in the presence of these ligand combinations (data not shown). The substantial effect of P_i with ATP without pyruvate is counter to the trend of minimal effects of P_i on fluorescence quenching with ATP. Based on fluorescence quenching results,[2] pyruvate was subsaturating at 100 μM with 100 μM ATP and 20 mM P_i (see below).

In potassium phosphate buffer, 5 mM pyruvate caused some reduction in PDHK2 binding to GST-L2 (*23*). Without P_i, 3 and 10 mM pyruvate (Supporting Information, Figure 1S), caused a somewhat smaller reduction in complex formation. Even though P_i weakens pyruvate binding[2], P_i acts with bound pyruvate in reducing PDHK2 binding to GST-L2; however, the decrease in K_d is small (~2-fold, and ~5-fold in total) in comparison to the weakening in binding when ATP and ADP were also included (>50-fold decrease in K_d required).

These ligands whether added alone or in combination, had qualitatively similar effects in reducing the lower level of PDHK2•GST-L2 complex formation in the presence of 50 mM NH_4^+ (Figure 2S). Under all conditions, 20 mM P_i greatly enhanced interference with complex formation. That contrasts with P_i in combination with NH_4^+ enhancing fluorescence quenching only with ADP and pyruvate[2]. Again, the full set of ligands (P_i, ATP or ADP, and pyruvate) was particularly effective in reducing binding of PDHK2 to GST-L2. Therefore, NH_4^+ is much less effective than K^+ in supporting complex formation, but NH_4^+ supported ligand-induced interference with binding of PDHK2 to the L2 domain.

P_i Effect on changes in PDHK2 Tetramer Formation. In potassium phosphate buffer, we reported that PDHK2 dimer self-associates to form a tetramer in the presence of pyruvate and ADP (or ATP) (*23*); a K_d of ~7.5 μM PDHK2 was determined for this interaction from sedimentation velocity and equilibrium studies using a range of PDHK2 concentrations (*23*). Even at concentrations as high as 31 μM PDHK2, no tetramer formation was observed in the absence of these ligands (*23*). Here we evaluate the self-association of 5.3 μM PDHK2 in the presence of 50 mM K^+ and 100 μM ADP or ATP with 100 μM pyruvate in the absence and presence of 20 mM P_i. Some tetramer forms in the absence of P_i (more so with ADP than ATP) but much more tetramer is formed when 20 mM P_i is also included (Figure 4). With ADP, pyruvate and 20 mM P_i the extent of tetramer formation was somewhat less than that observed with the same PDHK2, ADP and pyruvate concentrations in potassium phosphate buffer suggesting the equilibrium binding constant is slightly higher with 2.5-fold lower P_i. Our studies using fluorescence quenching (*23*)[2], indicate that the PDHK2•ADP•K^+•pyruvate•P_i complex is stabilized by K^+-dependent coupled binding of these ligands. We conclude that this pentanary complex induces one or more conformation that greatly enhances self-association of PDHK2 dimer. P_i appears to play a critical role in inducing/stabilizing the required conformational change(s). This equilibrium probably hinders PDHK2 binding to GST-L2. On the other hand, extensive ligand-induced interference with binding of PDHK2 to GST-L2 occurs at low protein concentrations in which there is limited tetramer formation (*23*). In the other direction at higher protein levels, GST-L2 has some capacity to hinder tetramer formation because, even with the greatly weakened binding of PDHK2 dimer to GST-L2 with the full set of ligands, there is less tetramer formation (bottom panels in Figure 3) than expected on the basis of the results in Figure 4. The physiological relevance of tetramer formation is considered in the Discussion.

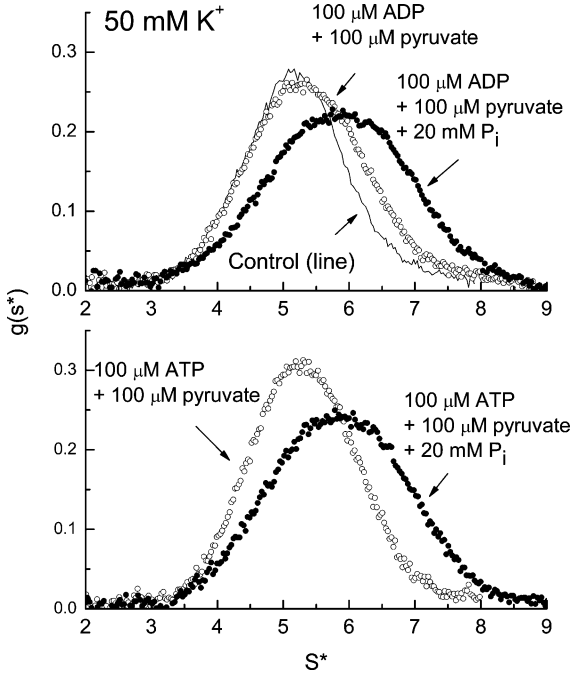

FIGURE 4: Effects of P_i on ligand-induced self-association of PDHK2 dimers. With ADP and pyruvate or ATP and pyruvate levels at 100 μM, the change in the sedimentation velocity pattern of 5.3 μM PDHK2 dimer in the absence and presence of 20 mM P_i is shown. Data were analyzed as described under Experimental Procedures with corrections for changes in buffer density and viscosity.

GST-L2 Effects on Ligand Binding and Effects of Ions. As shown in Figure 3S (Supporting Information), the Trp fluorescence by the combination of PDHK2 and GST-L2 proteins was close to the sum of the fluorescence intensities (320−420 nm) of the individual proteins. Under conditions in which >90% of PDHK2 is associated with GST-L2 with reduced lipoyl groups, the $L_{0.5}$ for ATP was increased by GST-L2 from 1.5 μM to 5.0 μM in studies using 50 mM

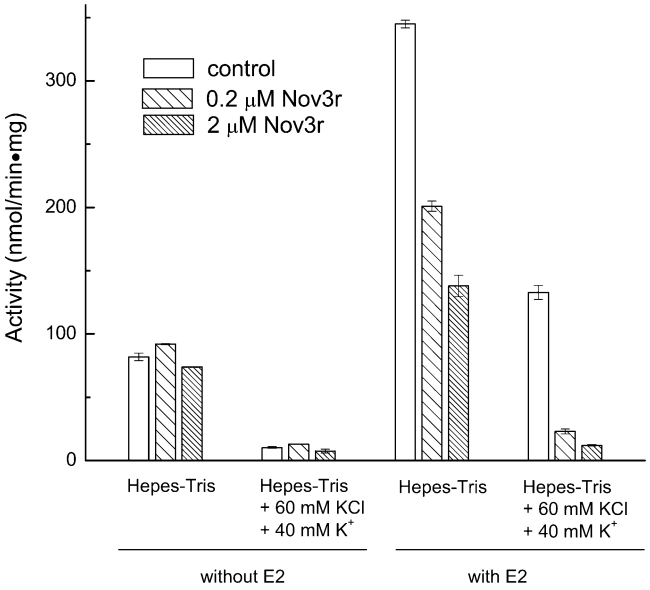

FIGURE 5: Effect of Nov3r on PDHK2 activity in the presence or absence of E2 with and without elevated K^+ and Cl^-. PDHK2 activity was measured by the standard ^{32}P-phosphate incorporation assay using assay conditions described under Experimental Procedures, which invariably include 13 mM P_i. Control assays in each set were performed with and without DMSO (0.5%); the full set of values were averaged because the activities were within experimental error. The level of PDHK2 was 0.15 μg in assays with E2 and 0.3 μg in assays without E2.

potassium phosphate buffer (Figure 4SA, Supporting Information). The latter is within experimental error, the same as the "K_d" estimated for ATP binding by PDHK2 associated with E2 using a cold trap procedure also using the same potassium phosphate buffer (*22*). Using a different buffer and isothermal calorimetry, Tunganova and Popov (*49*) derived a larger increase in the K_d for ATP from 1.6 μM to 12 μM with inclusion of 40 μM L2 monomer that was also treated with 5 mM dithiothreitol. We find that GST-L2 binding increased the $L_{0.5}$ for ADP from 12 to 46 μM (Figure 4SB). With 100 mM K^+, there was little effect on ADP binding without P_i included and, with 100 μM pyruvate also included, the tight binding of ADP was decreased by only 2-fold (Figure 5SA). With 100 mM K^+ and 20 mM P_i, GST-L2 also caused nearly a 4-fold increase in $L_{0.5}$ for pyruvate from ~5 μM to ~25 μM in the presence of 100 μM ADP but had a smaller change in the absence of ADP or absence of P_i (Figure 5SB and other results, Supporting Information). It seems likely that much of the P_i-dependent effects of GST-L2 in reducing the coupled ADP and pyruvate binding are due to binding interactions of the lipoyl prosthetic group of L2.

Effects of Nov3r on PDHK2 Activity and Lipoyl Domain Binding. Lipoamide or even lipoyl-peptides with the lipoyl group reduced and acetylated bind to PDHK2 too weakly to evaluate their effects. Effects of these structures on activity can be observed with PDHK3 (*50*). The affinity and requirements for Nov3r inhibiting PDHK2 activity by binding at the lipoyl group binding site were evaluated. In the absence of E2, there was minimal inhibition by 2 μM Nov3r of PDHK2 activity in the presence or absence of K^+. Inclusion of elevated K^+ markedly reduces PDHK2 activity in the absence of E2 (Figure 5). In the presence of E2, weak inhibition is observed in the absence of K^+ with 2 μM Nov3 causing only 60% inhibition (Figure 5). However, 2 μM Nov3r caused 91 ± 1% inhibition with 100 mM K^+ using a MOPS-K buffer that also contained 13 mM P_i and 60 mM Cl^-. Higher levels of Nov3r did not cause greater inhibition. With E2 and elevated K^+, 0.2 μM Nov3r gave 83% inhibition (Figure 5), which was 91% of the maximum inhibition observed with 2 μM Nov3r. Because 65 nM PDHK2 (130 nM binding sites) was used in these assays, occupancy of 91% of Nov3r binding sites would reduce free Nov3r to about 80 nM. This suggests that Nov3r binds with an affinity below 10 nM.

To obtain a better measure of the IC50 for Nov3r PDHK2, assays were conducted under conditions in which the inhibitor exceeded the level of PDHK2. PDHK2 activity was evaluated using low component levels and measuring PDHK2-catalyzed inactivation of PDC as described under Experimental Procedures. Under these assay conditions, 1.2 nM PDHK2 reversibly binds to 0.29 nM E2•E3BP (14 nM E2 subunits) with only about 15% of PDHK2 bound (*21*). Whereas with high concentrations of complex (^{32}P-phosphate incorporation assay above), PDHK2 activity at near saturating Nov3r (2 μM) was reduced to ~9%, it is reduced to 2.5 ± 1% under these assay conditions.[3] Again the latter corresponds to the ratio of control rates of PDHK2 activity determined without and with E2 under these dilute conditions (i.e., PDHK2 inactivated free E1 at 2.1 ± 0.9% as fast as it inactivated E2-bound E1).[3] Nov3r caused half-maximal inactivation of PDHK2 activity at 8.5 ± 0.5 nM (Figure 6); correcting the free Nov3r concentration for binding to 1.2 nM PDHK2 reduces this to ~7.8 nM[4]. Similar potent inhibition was observed with AZD7545 and other related compounds provided by AstraZeneca (*31*).[5] Using a higher level of rat PDHK2 (~220 nM), an IC50 of ~110 nM AZD7545 was obtained probably due to titration of PDHK2 with the tight-binding AZD7545 (*52*).

As shown in Figure 7, 20 μM Nov3r (lower panel) completely prevented binding of 4.3 μM PDHK2 to 5.7 μM GST-L2. Binding of PDHK2 to the E2 60mer was also prevented (data not shown). This is consistent with the binding of Nov3r at the lipoyl binding site (*26*); prior studies established that the lipoyl prosthetic group makes a critical contribution to lipoyl domain binding by PDHK (*14*, *25*, *50*, *53*, *54*). With rat PDHK2, evidence for the Nov3r-related AZD7545 interfering with PDHK2 binding to GST-L2 was

[3] With free PDHK2 phosphorylating free E1, PDHK2 has a very high K_m for E1 (*22*) and the specific activity falls off steeply as E1 is diluted from ~2.6 μM (standard assay conditions giving ~8% rate with E2 with free E1) to 0.065 μM E1 used in these dilute assays. In contrast, with E2-bound PDHK2 (K_d = 0.4 μM (*21*)) phosphorylating E2-bound E1 (K_d for up to 20 E1 bound ~0.03 μM and even tighter for first six (*51*)), there is a much smaller (~7.5-fold) fall off in the specific activity of PDHK2, which primarily reflects the fraction of E2-bound PDHK2. The fraction of bound PDHK2 is estimated as ~0.15 with the concentration of components used.

[4] Inhibition should be achieved by just one Nov3r molecule binding to PDHK2 dimer because this should prevent the tight bifunctional binding of PDHK2 to E2, which would be required at the low concentration of complex used in these studies. This conclusion is based on the much tighter binding of PDHK2 dimer to GST-L2 (or E2) than to the L2 monomer (*21*). Figure 6 shows the added concentration. When half the PDHK2 dimers have no Nov3r bound, random binding at independent binding sites leads to 20.6% of the remaining 50% of dimers having two Nov3r bound.

[5] Xiaohua Yan, Thomas E. Roche, Roger J. Butlin, and Rachel M. Mayers, unpublished work.

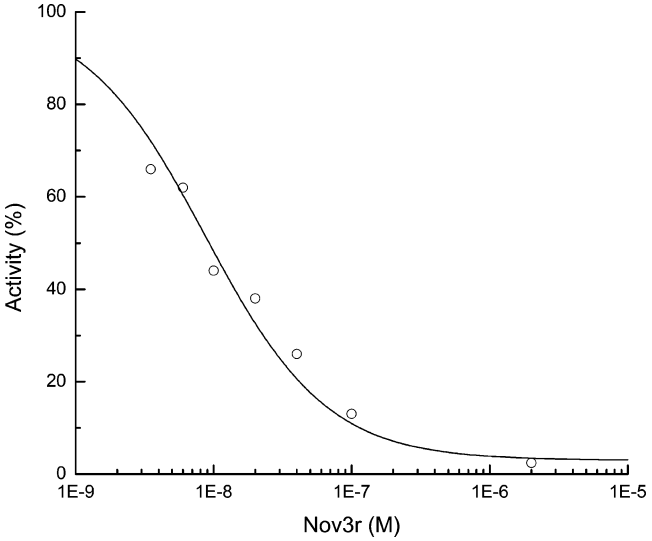

FIGURE 6: Concentration dependence for Nov3r inhibition PDHK2 activity. PDHK2 (1.2 nM) catalyzed inactivation of reconstituted PDC was measured as described under Experimental Procedures. The data were fit by the equation: % activity = $((100 - B{\cdot}0.85)/(1 + I/K_i)) + B{\cdot}0.85 + (B{\cdot}0.15(1 - (K_i/(K_i + I))$, where B is % activity of free PDHK2 (85% free initially) and K_i is the inhibition constant for Nov3r (I) inhibition of E2-activated PDHK2 activity (97% activity by 15% PDHK2 bound to E2 initially). The data were fit with $K_i = 8.5$ nM and $B = 3\%$[3]. This equation treats the removal of E2-activated PDHK2 activity (97% of the initial activity; IC50 at loss 48.5% activity) with a noncompetitive inhibition format with an equivalent gain of 15% of the low activity of free PDHK2 as the kinase is dislodged from E2 due to Nov3r binding.

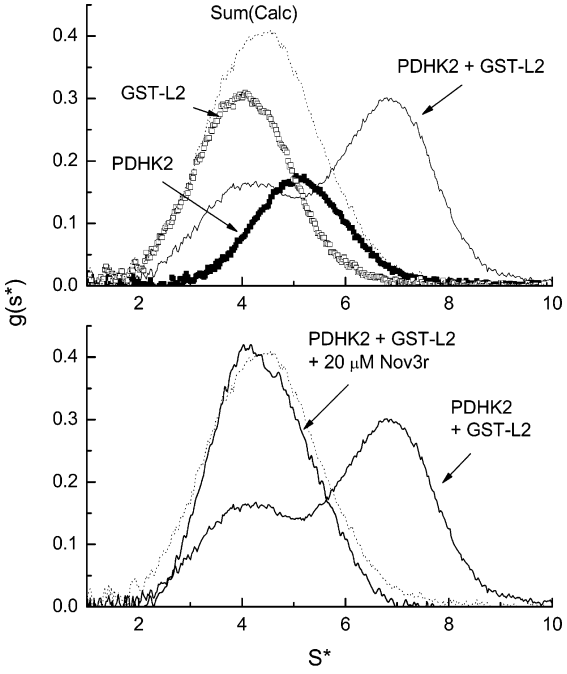

FIGURE 7: Nov3r prevention of PDHK2 binding to GST-L2. The upper panel shows $g(s^*)$ profile for sedimentation velocity of individual components in the presence of Nov3r and for 4.3 μM PDHK2 and 5.7 μM GST-L2 in the absence of Nov3r (repeated in the lower panel). The lower panel shows the $g(s^*)$ profile of the same levels of PDHK2 and GST-L2 in the presence of 20 μM Nov3r. Also shown are the sum of the $g(s^*)$ profiles for PDHK2 and GST-L2 alone (dotted lines both panels). Sedimentation velocity was conducted in 50 mM potassium phosphate buffer containing 0.5 mM EDTA and 5 mM dithiothreitol.

recently described (*53*). Nov3r did not foster PDHK2 forming a tetramer and had a small effect in hindering tetramer formation (data not shown) that is explained by effects of Nov3r on ligand binding (below).

Effect of Nov3r on Ligand-Induced Trp-Fluorescence Quenching of PDHK2 and Coupling to P_i Binding. As described elsewhere (*4*, *26*), Nov3r appears to be an analog of the acetyl-dihydrolipoyl group. Nov3r, alone, had no effect on Trp fluorescence in the presence or absence of K^+. However, ligand-induced changes in Trp fluorescence can readily be observed with fully saturated binding of Nov3r. We have presented evidence that reductive acetylation speeds up dissociation of ADP and that this means of stimulating PDHK2 activity requires not only K^+ but also anions (Cl^- or P_i, with the largest fractional increase in PDHK2 activity with both) (*20*). Nov3r did not significantly change the concentration dependence for K^+/ATP-dependent quenching of Trp fluorescence when either K^+ or ATP was varied at fixed levels of the other with or without 20 mM P_i (Table 1S, Supporting Information). With ADP varied, there was a substantial change from P_i enhancing quenching and lowering $L_{0.5}$ for ADP or K^+ (companion paper[2]) to P_i hindering quenching and increasing the $L_{0.5}$ for these ligands with Nov3r bound (Figure 8A). In the presence of P_i, Nov3r increased the $L_{0.5}$ for ADP at different K^+ levels (Table 1) or the $L_{0.5}$ for K^+ with different ADP levels (Table 1S) by 1.6−1.8-fold along with decreasing in Q_{max}. This is consistent with binding at the lipoyl group binding site reducing ADP/K^+ binding at the distant active site by a P_i-dependent mechanism.

Nov3r had no detectable effect on the weak binding of pyruvate by PDHK2 in the presence of 100 mM K^+ and 20 mM P_i. There was minimal interference by Nov3r with the higher affinity pyruvate binding with 200 μM ADP and 100 mM K^+ (Table 1). However, the tight pyruvate binding with 100 mM K^+, 20 mM P_i and 200 μM ADP was markedly weakened by Nov3r with an 8-fold increase in $L_{0.5}$ (Figure 8C, Table 1). Under these conditions with 200 μM ADP, ~88 and ~82% of active sites of PDHK2 are predicted to bind ADP in the absence and presence of Nov3r, prior to addition of pyruvate. Therefore, the marked interference by Nov3r with pyruvate binding apparently occurs when K^+/ADP are bound at the active site and P_i is bound. When ADP was varied with 100 mM K^+ and 20 mM P_i and either 100 μM (Figure 8B) or 300 μM pyruvate, Nov3r weakened ADP binding causing ~6-fold increase in $L_{0.5}$ for ADP (Table 1). However, the $L_{0.5}$ of ADP with Nov3r remained lower than without pyruvate (3-fold with 300 μM pyruvate). Because of the weak binding by pyruvate with K^+/P_i in the absence of ADP, there was a substantial increase in pyruvate binding as the ADP level was increased. Although pyruvate binding increased even with Nov3r, a significant portion of the decrease in Q_{max} with Nov3r compared to the control is due to less pyruvate binding. We suggest that P_i plays a key role in transmitting the interfering signal of Nov3r to affect pyruvate binding and ADP binding at the active site. The transformation with ADP/K^+ to P_i-dependent reduction in binding of pyruvate with Nov3r rather than enhancing binding is not due to the decrease in ADP binding. Two alternatives may explain Nov3r interfering with the capacity of ADP and P_i to strengthen pyruvate binding. One possibility is that allosterically coupled P_i and Nov3r binding hinders binding at the pyruvate binding site and the active site.

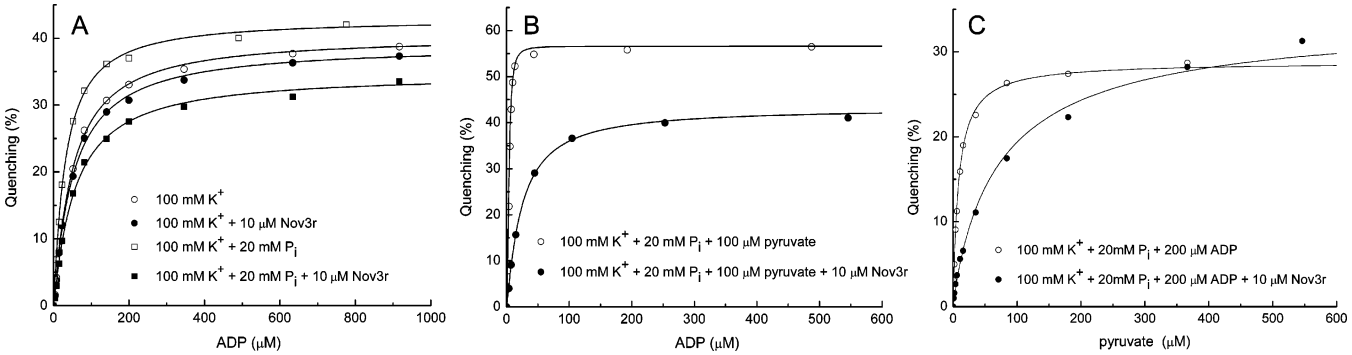

FIGURE 8: Effects of Nov3r on fluorescence quenching by ADP in the presence and absence of P_i (panel A), by ADP in the presence of P_i and pyruvate (panel B), and by pyruvate in the presence of P_i and ADP (panel C). Fluorescence excitation was at 295 nm and the fluorescence measured at 320−420 nm in mixtures containing 0.3 μM PDHK2, 2.0 mM Mg^{2+} and 100 mM K^+. Fixed ligands were added at the concentrations indicated in the insets in figure panels. Data are plotted as % quenching based on the initial fluorescence (0% quenching) after the addition of fixed ligands. Other condition and data analysis were as described under Experimental Procedures in this and the companion paper.[2]

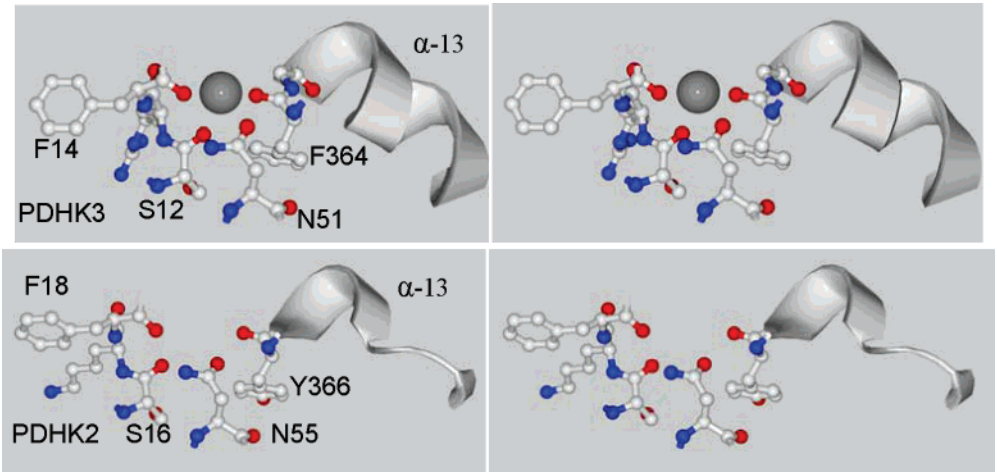

FIGURE 9: Stereoviews of K^+ binding site on the trough side of PDHK3 and equivalent structure of the aligned residues in PDHK2. The only change in chelating residues is a conservative substitution of Tyr366 in PDHK2 for Phe364 in PDHK2. Residue numbering is as indicated in Figure 1.

Alternatively, Nov3r may greatly hinders P_i binding and therefore removes the positive effects of P_i on ADP/pyruvate binding.

To evaluate this further, P_i was varied in the presence of 100 mM K^+ and 100 μM ADP (Figure 6SA, Supporting Information) and with those ligands plus 100 μM pyruvate (Figure 6SB) in the presence and absence of Nov3r. With just ADP, the pattern of increasing P_i causing a transition from decreasing to increasing fluorescence (described in the companion paper[2]) was favored with Nov3r at lower levels of P_i. These data suggest that P_i binding at a second site is enhanced by Nov3r.

With 100 μM pyruvate also included (Figure 6SB), Nov3r caused an immediate transition from fluorescence quenching to increased fluorescence with the level of P_i. As explained under Supporting Information, this transition due to Nov3r for the interval from 0 to 20 mM P_i can be attributed to the change that Nov3r causes in PDHK2 binding of ADP and pyruvate (Table 1). We conclude the interfering effects of Nov3r on pyruvate and ADP binding are greatly enhanced by P_i due to coupled binding of Nov3r and P_i. These results indicate that PDHK2-bound P_i plays an important role in the transmission of regulatory effects from the lipoyl group binding site.

DISCUSSION

We previously reported a strong correlation between the effects of ligands in quenching Trp fluorescence and in reducing binding of PDHK2 to the GST-L2 dimer containing reduced lipoyl groups (*23*). Furthermore, the combination of ADP and pyruvate caused the PDHK2 dimer to associate and form a tetramer (*23*). Here we find that K^+ aids binding of PDHK2 to GST-L2 and that ligand interference with binding to the L2 domain is K^+ dependent. However, in contrast to ligand effects on fluorescence quenching[2], the NH_4^+ ion was not effective in replacing the K^+ ion in aiding binding of PDHK2 to GST-L2, but NH_4^+ did promote ligands interfering with the limited complex that was formed. These observations indicate that K^+ is acting at a second site in facilitating L2 binding to PDHK2 and that binding of K^+ at both sites is required for ligand-induced interference with GST-L2 binding. The PDHK3•L2 structure (*27*) (Figure 1) reveals that K^+ is bound at a site that is conserved in PDHK2 (Figure 9). The Phe14 side chain of PDHK3 directly interacts with Leu140 of the L2 domain; the K^+ binding site is equidistant between the Trp that anchors the cross arm and the lipoyl group binding site. Phe364 of PDHK3 precedes the short helix 13, which contains three residues (conserved in PDHK2) that interact with the L2 domain. This conserved

Table 1: Effects of Nov3r on Binding of Ligands to PDHK2[a]

fixed ligand conditions	varied ligand	$L_{0.5}$ (n_H)[c] of varied ligand (mM)		$L_{0.5}$(+Nov3r)/ $L_{0.5}$(−Nov3r)	ΔQ_{max} (+Nov3r)
		control	+Nov3r		
					Δ%
none	ADP[b]	1010 ± 40	1350 ± 20	1.3	−3
100 mM K^+	ADP	47.5 ± 2.4	46.8 ± 1.7	1.0	−1
100 mM K^+, 20 mM P_i	ADP	25 ± 1	44.5 ± 3	1.8	−6.5
50 mM K^+, 20 mM P_i	ADP	35 ± 3	54.5 ± 4.5	1.55	−8
5 mM K^+, 20 mM P_i	ADP	225 ± 20	360 ± 35	1.6	−7
20 mM P_i	ADP[a]	2300 ± 255	2680 ± 290	1.15	−4
100 mM K^+, 100 μM Pyr	ADP	11 ± 2 (1.3)	56.5 ± 1.5	5.0	−2.5
100 mM K^+, 20 mM P_i, 100 μM Pyr	ADP	3.9 ± 0.1 (2.1)	24.0 ± 0.6	6.1	−7
100 mM K^+, 20 mM P_i, 300 μM Pyr	ADP	2.7 ± 0.07 (2.6)	14.5 ± 0.4 (1.3)	5.4	−7
100 mM K^+, 200 μM ADP	Pyr	18.3 ± 1.5 (0.89)	26.2 ± 1.7	1.4	−2
100 mM K^+, 20 mM P_i, 200 μM ADP	Pyr	8.3 ± 0.2	75.5 ± 3.5	9.1	+6[d]

[a] Most experiments were conducted with 2.0 mM Mg^{2+}; however, Mg^{2+} was increased to 6.0 mM[b] when varied ADP exceeded 800 μM. [b] Mg^{2+} was 6.0 mM. [c] The n_H values are included only when they differ from 1.0 by $>+0.20$ or <-0.1. [d] There was 2% decrease in Q_{tot} with Nov3r.

site would seem to be an excellent location for K^+ binding influencing L2 binding.

We also find that P_i has a pronounced effect in increasing ligand interference with PDHK2 binding to GST-L2 and PDHK2 dimer associating to a tetramer. P_i-enhancement of pyruvate binding was dependent upon inclusion of K^+ and ADP[2]. Similarly, the full set of ligands (K^+, ADP and pyruvate) was required for potent P_i-enhanced interference with PDHK2 binding to GST-L2 and P_i causing a marked increase in ligand-induced formation of PDHK2 tetramer. With these ligands, P_i bound to PDHK2 with an affinity of 0.85 mM[2]; free P_i in the mitochondrial matrix space can apparently increase to concentrations above this level (*55*−*57*).[6] It is likely that tetramer formation interferes with PDHK2 binding to GST-L2. However, nearly complete interference with PDHK2 binding to GST-L2 can be observed at concentrations of PDHK2 that form limited tetramer (*23*). Thus, it seems likely that the conformational transition that hinders GST-L2 binding may favor tetramer formation, but tetramer formation is not a requisite step for ligand binding hindering PDHK2 binding to L2.

Given the K_d of ∼7.5 μM for tetramer formation (*23*), at least a 10-fold stronger binding affinity would be needed for tetramer formation to be significant at the levels PDHK2 that are estimated in matrix space. Interactions that are weak with dilute protein concentrations are enhanced 10−100-fold at the high protein concentrations found in the mitochondrial matrix (>400 mg/mL (*58*, *59*)) when, as usually occurs, complex formation reduces molecular crowding (*60*, *61*). We have suggested that ligand-induced dislodging of the C-terminal cross-arm may contribute to reduced PDHK2 binding to the L2 domain and to the formation of the tetramer structure (*23*). We have found that ADP and pyruvate caused a marked P_i-dependent decrease in Trp fluorescence polarization that is consistent with greater Trp mobility.[7] Both Trp383 and Trp371 are located in the cross arm. Crystal structures indicate that closure of the active site cavity between the R and Cat domains may be linked to release of the cross arms with increased opening of the trough region between the subunits (*25*, *26*).

Both the L2 domain structure and the lipoyl prosthetic group contribute to L2 associating with PDHK (*3*, *14*, *19*, *20*, *21*, *25*, *48*−*50*, *52*−*54*). We found that Nov3r prevents binding of PDHK2 to GST-L2, which is in accord with this ligand and related AZD7545 occupying the lipoyl group binding site (*26*, *31*, *52*). We evaluated the ion requirements for and effects of binding of Nov3r at the lipoyl binding site on PDHK2 catalysis. Consistent with interference with E2 binding being the primary way Nov3r reduces PDHK2 activity, we have found that Nov3r only modestly inhibits the low activity in the absence of E2 but potently inhibits E2-activated PDHK2 activity. Indeed, Nov3r reduced PDHK2 activity to near the low levels observed in the absence of E2, which was ∼8% of the E2-enhanced PDHK2 activity at high component levels and ∼2.5% with dilute components. The potent and high affinity inhibition (IC50 = 7.8 nM) by Nov3r required inclusion of K^+ and anions (P_i and Cl^-). The ion requirements are in complete accord with the suggestion that Nov3r is a structural analog of acetyl-dihydrolipoamide (*3*). Effective stimulation of PDHK2 by reductive acetylation of the lipoyl groups of E2 requires these same ions (*20*). Additionally, all the Nov3r-related compounds that potently inhibit E2-activated PDHK2 activity stimulate the activity of the PDHK4 isoform (*4*, *31*);[5] that stimulation also requires K^+, P_i, and Cl^-. Given the distinguishing isoform properties of PDHK4 (*4*),[8] those results further support the concept that these inhibitors act as analogs of acetyl-dihydrolipoamide.

To further assess how interactions of Nov3r at the lipoyl group binding site influence the interactions of ligands at other sites in PDHK2, we evaluated the capacity of Nov3 to significantly change ligand-induced quenching of Trp fluorescence. As can be recognized in Figure 1, the lipoyl group (Nov3r) binding site is located a substantial distance from the active site with the DCA/pyruvate site located in-between (*25*, *26*). Communication to the active site is of particular

[6] ^{31}P NMR measurements most accurately measure cytoplasmic P_i (*55*) although evidence for direct NMR detection of matrix P_i has been described (*56*); the cytoplasmic level can be used to estimate intramitochondrial P_i based on thermodynamic equilibria (*55*) or the ratio of P_i maintained outside to inside mitochondria (up to 10 times higher inside) (*57*). Matrix P_i concentrations of 1.0−2.5 mM are indicated.

[7] Yasuaki Hiromasa, Liangyan Hu, Thomas E. Roche, unpublished work.

[8] PDHK4 has high activity in the absence of E2 because PDHK4 has a much lower K_m for free E1 (*4*, *62*). Although PDHK4 activity is minimally enhanced by E2, reductive acetylation of E2 does stimulate PDHK4 activity (*4*, *62*, *63*). Potentially contributing to the unique response of PDHK4 to Nov3r, PDHK4 is the only PDHK isoform with any amino acid difference in the R domain lipoyl (Nov3r) binding site (Phe28 of PDHK2 is replaced with aligned Leu32 in PDHK4).

interest because acetylation of the L2 domain of E2 is suggested to stimulate PDHK2 activity by speeding up ADP dissociation (*20*). We were also particularly interested in the roles of K^+ and P_i because these ions are needed for significant stimulation by reductive acetylation.

In the absence of P_i, Nov3r had minimal effects on the binding of ATP, ADP or K^+ by PDHK2 as assessed by Trp-fluorescence quenching. P_i effects changed from increasing Q_{max} and enhancing ADP binding to reducing Q_{max} and reducing ADP binding with Nov3r (Figure 8A). With inclusion of 20 mM P_i, 10 μM Nov3r only caused 1.5−2-fold increases in $L_{0.5}$ for ADP or K^+ with lesser effects on ATP binding. However, when either ADP or pyruvate was varied with the other ligand held at a fixed level, Nov3r caused large (6−9-fold) increases in the $L_{0.5}$ values for these ligands; again this required inclusion of both 100 mM K^+ and 20 mM P_i. For conveying the transforming effects of Nov3r on ADP and pyruvate binding, it seems likely that the strong K^+- and P_i-dependent linkage between bound ADP and pyruvate is altered by a P_i-supported coupling. The obvious choice for coupling is between the pyruvate and the adjacent Nov3r binding site, in which case weakened ADP binding might be a secondary effect of Nov3r weakening pyruvate binding. However, in the absence of ADP with 100 mM K^+ and 20 mM P_i, Nov3r had no detectable effect on pyruvate binding, whereas, in the absence of pyruvate, Nov3r increased the $L_{0.5}$ of PDHK2 for ADP as indicated above.

Therefore, the effects of P_i were transformed from greatly aiding the coupled binding of ADP and pyruvate to facilitating Nov3r-induced reduction in ADP and pyruvate binding to PDHK2. This transition is exemplified when the P_i level was varied by the marked change from fluorescence being quenched to being enhanced with inclusion of Nov3r (Figure 6SB). Even though these changes in fluorescence with Nov3r seem to be attributable primarily to changes in ADP and pyruvate binding as the P_i level was increased, titration of P_i with ADP and K^+ produces a complex response that does not seem to be due just to changes in ADP binding. Introduction of Nov3r minimized the initial fluorescence quenching phase and enhanced the fluorescence increase at higher levels of P_i. Thus, the present studies reveal complexities in K^+ and P_i binding that suggest the involvement of multiple P_i binding sites. Obtaining a PDHK2 crystal structure with K^+, ADP, pyruvate, and P_i bound (dimer or tetramer) with and without Nov3r would be particularly helpful for understanding the structural basis for these important ligand-induced regulatory transitions.

Previously, it was known that P_i enhanced pyruvate inhibition of PDHK (*22*, *64*) and P_i also aided stimulation of PDHK by reductive acetylation (*12*, *20*). In the companion paper[2], we find P_i hinders pyruvate binding in the absence of ADP but greatly strengthens pyruvate binding with ADP. Here, we have demonstrated that P_i markedly increases the capacities of ADP and pyruvate to interfere with PDHK2 binding to GST-L2 and to support PDHK2 tetramer formation. Additionally P_i greatly enhances communication of the effects of Nov3r in reducing ADP and pyruvate binding. Thus, the binding of ADP and pyruvate along with K^+ is a common requirement for P_i potently altering coupled ligand binding and fostering the transmission of major conformational changes that alter protein interactions. Results with PDHK2 mutants[7] are consistent with P_i binding in the active site cavity in a position in which it may form a bridging interaction between the R and Cat domains. PDHK2 crystal structures supporting this binding location are needed.

ACKNOWLEDGMENT

We thank Michal Zolkiewski and the Department of Biochemistry at Kansas State University for continued maintenance of the Optima XL-I ultracentrifuge used in these studies.

SUPPORTING INFORMATION AVAILABLE

Effects of pyruvate on PDHK2 binding to GST-L2 with 100 mM K^+ (Figure 1S); support by 50 mM NH_4^+ in ligands weakening binding of PDHK2 to GST-L2 (Figure 2S); fluorescence spectra of GST-L2, PDHK2, and the combination of these proteins (Figure 3S); effect of GST-L2 on Trp fluorescence quenching by ATP and ADP (Figure 4S); effects of GST-L2 with or without 20 mM P_i on the coupled binding of ADP and pyruvate (Figure 5S); effects of Nov3r on binding of K^+ and adenine nucleotides by PDHK2 (Table 1S); and effects of Nov3r on fluorescence quenching by P_i in the presence of ADP or ADP plus pyruvate (Figure 6S). This information is available free of charge via the Internet at http://pubs.acs.org.

REFERENCES

1. Randle, P. J. (1986) Fuel selection in animals, *Biochem. Soc. Trans. 14*, 1799−1806.
2. Randle, P. J. (1995) Metabolic fuel selection: general integration at the whole-body level, *Proc. Nutr. Soc. 54*, 317−327.
3. Roche, T. E., Baker, J. C., Yan, X., Hiromasa, Y., Gong, X., Peng, T., Dong, J., Turkan, A., and Kasten, S. A (2001) Distinct regulatory properties of pyruvate dehydrogenase kinase and phosphatase isoforms, *Prog. Nucleic Acid Res. Mol. Biol. 70*, 33−75.
4. Roche, T. E., and Hiromasa, Y. (2007) Pyruvate dehydrogenase kinase regulatory mechanisms and inhibition in treating diabetes, heart ischemia, and cancer, *Cell. Mol. Life Sci. 64*, 830−849.
5. Sugden, M. C., and Holness, M. J. (2003) Recent advances in mechanisms regulating glucose oxidation at the level of the pyruvate dehydrogenase complex by PDKs, *Am. J. Physiol. Endocrinol. Metab. 284*, E855−E862.
6. Reed, L. J. (1974) Multienzyme complexes, *Acc. Chem. Res. 7*, 40−46.
7. Pettit, F. H., Pelley, J. W., and Reed, L. J. (1975) Regulation of pyruvate dehydrogenase kinase and phosphatase by acetyl-CoA/CoA and NADH/NAD ratios, *Biochem. Biophys. Res. Commun. 65*, 575−582.
8. Kerbey, A. L., Randle, P. J., Cooper, R. H., Whitehouse, S., Pask, H. T., and Denton, R. M. (1976) Regulation of pyruvate dehydrogenase in rat heart. Mechanism of regulation of proportions of dephosphorylated and phosphorylated enzyme by oxidation of fatty acids and ketone bodies and of effects of diabetes: role of coenzyme A, acetyl-coenzyme A and reduced and oxidized nicotinamide-adenine dinucleotide, *Biochem. J. 154*, 327−348.
9. Batenburg, J. J., and Olson, M. S. (1976) Regulation of pyruvate dehydrogenase by fatty acid in isolated rat liver mitochondria, *J. Biol. Chem. 251*, 1364−1370.
10. Hansford, R. G. (1976) Studies on the effects of coenzyme A-SH: acetyl coenzyme A, nicotinamide adenine dinucleotide: reduced nicotinamide adenine dinucleotide, and adenosine diphosphate: adenosine triphosphate ratios on the interconversion of active and inactive pyruvate dehydrogenase in isolated rat heart mitochondria, *J. Biol. Chem. 251*, 5483−5489.
11. Randle, P. J. (1998) Regulatory interactions between lipids and carbohydrates: the glucose fatty acid cycle after 35 years, *Diabetes Metab. Rev. 14*, 263−283.
12. Cate, R. L., and Roche, T. E. (1978) A unifying mechanism for stimulation of mammalian pyruvate dehydrogenase kinase activity by NADH, dihydrolipoamide, acetyl Coenzyme A, or pyruvate, *J. Biol. Chem. 253*, 496−503.

13. Rahmatullah, M., and Roche, T. E. (1985) Modification of bovine kidney pyruvate dehydrogenase kinase activity by CoA esters and their mechanism of action, *J. Biol. Chem. 260*, 10146−10152.
14. Ravindran, S., Radke, G. A., Guest, J. R., and Roche, T. E. (1996) Lipoyl domain-based mechanism for integrated feedback control of pyruvate dehydrogenase complex by enhancement of pyruvate dehydrogenase kinase activity, *J. Biol. Chem. 271*, 653−662.
15. Popov, K. M. (1997) Regulation of mammalian pyruvate dehydrogenase kinase, *FEBS Lett. 419*, 197−200.
16. Thekkumkara, T. J., Ho. L., Wexler, I. D., Pons, G., Lui, T-C., and Patel, M. S. (1988) Nucleotide sequence of a cDNA for the dihydrolipoamide acetyltransferase component of human pyruvate dehydrogenase complex, *FEBS Lett. 240*, 45−48.
17. Harris, R. A., Bowker-Kinley, M. M., Wu, P., Jeng, J., and Popov, K. M. (1997) Dihydrolipoamide dehydrogenase-binding protein of the human pyruvate dehydrogenase complex. DNA-derived amino acid sequence, expression, and reconstitution of the pyruvate dehydrogenase complex, *J. Biol. Chem. 272*, 19746−19751.
18. Yang, D., Gong, X., Yakhnin, A., and Roche, T. E. (1998) Requirements for the adaptor protein role of dihydrolipoyl acetyltransferase in the upregulated function of the pyruvate dehydrogenase kinase and pyruvate dehydrogenase phosphatase, *J. Biol. Chem. 273*, 14130−14137.
19. Baker, J. C., Yan, X., Peng, T., Kasten, S. A., and Roche, T. E. (2000) Marked differences between two isoforms of human pyruvate dehydrogenase kinase, *J. Biol. Chem. 275*, 15773−15781.
20. Bao, H., Kasten, S. A., Yan, X., Hiromasa, Y., and Roche, T. E (2004) Pyruvate dehydrogenase kinase isoform 2 activity stimulated by speeding up the rate of dissociation of ADP, *Biochemistry 43*, 13442−13451.
21. Hiromasa, Y., and Roche, T. E. (2003) Facilitated interaction between the pyruvate dehydrogenase kinase isoform 2 and the dihydrolipoyl acetyltransferase, *J. Biol. Chem. 278*, 33681−33693.
22. Bao, H., Kasten, S. A., Yan, X., and Roche, T. E. (2004) Pyruvate dehydrogenase kinase isoform 2 activity limited and further inhibited by slowing down the rate of dissociation of ADP, *Biochemistry 43*, 13432−13441.
23. Hiromasa, Y., Hu, L., and Roche, T. E. (2006) Ligand-induced effects on pyruvate dehydrogenase kinase isoform 2, *J. Biol. Chem. 281*, 12568−12579.
24. Steussy, N. C., Popov, K. M., Bowker-Kinley, M. M., Sloan, R. B., Harris, R. A., and Hamilton, J. A. (2001) Structure of pyruvate dehydrogenase kinase. Novel folding pattern for a serine protein kinase, *J. Biol. Chem. 276*, 37443−37450.
25. Kato, M., Chuang, J. L., Tso, S-C., Wynn, R. M., and Chuang, D. T. (2005) Crystal structure of pyruvate dehydrogenase kinase 3 bound to lipoyl domain 2 of human pyruvate dehydrogenase complex, *EMBO J. 24*, 1763−1774.
26. Knoechel, T. R., Tucker, A. D., Robinson, C. M., Phillips, Taylor, C. W., Bungay, P. J., Kasten, S. A., Roche, T. E., and Brown, D. G. (2006) Regulatory roles of the N-terminal domain based on crystal structures of human pyruvate dehydrogenase kinase 2 containing physiological and synthetic ligands, *Biochemistry 45*, 402−415.
27. Devedjiev, Y., Steussy, C. N., Vassylyev, D. G. (2007) Crystal Structure of an Asymmetric Complex of Pyruvate Dehydrogenase Kinase 3 with Lipoyl Domain 2 and its Biological Implications, *J. Mol. Biol. 370*, 407−416.
28. Aicher, T. D., Anderson, R. C., Beberntiz, G. R., Coppola, G. M., Jewell, C. F., Knorr, D. C., Liu, C., Sperbeck, D. M., Brand, L. J., Strohschein, R. J., Gao, J., Vinluan, C. C., Shetty, S. S., Dragland, C., Kaplan, E. L., DelGrande, D., Islam, A., Liu, X., Lozito, R. J., Maniara, W. M., Walter, R. E., and Mann, W. R. (1999) (R)-3,3,3-trifluoro-2-hydroxy-2-methylpropionamides are orally active inhibitors of pyruvate dehydrogenase kinase, *J. Med. Chem. 42*, 2741−2746.
29. Aicher, T. D., Anderson, R. C., Gao, J., Shetty, S. S., Coppola, G. M., Stanton, J. L., Knorr, D. C., Sperbeck, D. M., Brand, L. J., Winluan, C. C., Kaplan, E. L., Dragland, C. J., Tomaselli, H. C., Islam, A., Lozito, R. J., Liu, X., Maniara, W. M., Fillers, W. S., DelGrande, D., Walter, R. E., and Mann, W. R. (2000) Secondary amides of (R)-3,3,3-trifluoro-2-hydroxy-2-methylpropionic acid as inhibitors of pyruvate dehydrogenase kinase, *J. Med. Chem. 43*, 236−249.
30. Bebernitz, G. R., Aicher, T. D., Stanton, J. L., Gao, J., Shetty, S. S., Knorr, D. C., Strohschein, R. J., Tan, J., Brand, L. J., Liu, C., Wang, W. H., Vinluan, C. C., Kaplan, E. L., Drangland, C. J., DelGrande, D., Islam, A., Lozito, R. J., Liu, X., Maniara, W. M., and Mann, W. R. (2000) Anilides of (R)-trifluoro-2-hydroxy-2-methylpropionic acid as inhibitors of pyruvate dehydrogenase kinase, *J. Med. Chem. 43*, 2248−2257.
31. Morrell, J. A., Orme, J., Butlin, R. J., Roche, T. E., Mayers, R. M., and Kilgour, E. (2003) AZD7545 is a selective inhibitor of pyruvate dehydrogenase kinase 2, *Biochem. Soc. Trans. 31*, 1168−1170.
32. Hutson, S., and Randle, P. J. (1978) Enhanced activity of pyruvate dehydrogenase kinase in rat heart mitochondria in alloxan-diabetes or starvation, *FEBS Lett. 92*, 73−76.
33. Wu, P., Inskeep, K., Bowker-Kinley, M. M., Popov, K. M., and Harris, R. A. (1999) Mechanism responsible for inactivation of skeletal muscle pyruvate dehydrogenase complex in starvation and diabetes, *Diabetes 48*, 1593−1599.
34. Harris, R. A., Huang, B., and Wu, P. (2001) Control of pyruvate dehydrogenase kinase gene expression, *Adv. Enzyme Regul. 41*, 269−288.
35. Kwon, H-S., and Harris, R. A. (2004) Mechanisms responsible for the regulation of pyruvate dehydrogenase kinase 4 gene expression, *Adv. Enzyme Regul. 44*, 109−121.
36. Mayers, R. M., Butlin, R. J., Kilgour, E., Leighton, B., Martin, D., Myatt, J., Orme, J. P., Holloway, B. R. (2003) AZD7545, a novel inhibitor of pyruvate dehydrogenase kinase 2 (PDHK2), activates pyruvate dehydrogenase in vivo and improves blood glucose control in obese (fa/fa) Zucker rats, *Biochem. Soc. Trans. 31*, 1165−1167.
37. Mayers, R. M., Leighton, B., Butlin, R. J., and Kilgour, E. (2005) PDK kinase inhibitors: a novel therapy for Type II diabetes, *Biochem. Soc. Trans. 33*, 367−370.
38. Hiromasa, Y., Fujisawa, T., Aso, Y., and Roche, T. E. (2004) Organization of the cores of the mammalian pyruvate dehydrogenase complex formed by E2 and E2 plus the E3-binding protein and capacities to bind the E1 and E3 components, *J. Biol. Chem. 279*, 6921−6933.
39. Liu, S., Baker, J. C., Andrews, P. C., and Roche, T. E. (1995) Recombinant expression and evaluation of the lipoyl domains of the dihydrolipoyl acetyltransferase component of human pyruvate dehydrogenase complex, *Arch. Biochem. Biophys. 316*, 926−940.
40. Liu, T-C., Korotchkina, L. G., Hyatt, S. L., Vettakkorumakankav, N. N., and Patel, M. S. (1995) Spectroscopic studies of the characterization of recombinant human dihydrolipoamide dehydrogenase and its site-directed mutants, *J. Biol. Chem. 270*, 15545−15550.
41. Turkan, A., Hiromasa, Y., and Roche, T. E. (2004) Formation of a complex of the catalytic subunit of pyruvate dehydrogenase phosphatase isoform 1 (PDP1c) and L2 domain forms a Ca^{2+}-binding site and captures PDP1c as a monomer, *Biochemistry 43*, 15073−15085.
42. Philo, J. S. (2000) A method for directly fitting the time derivative of sedimentation velocity data and an alternative algorithm for calculating sedimentation coefficient distribution functions, *Anal. Biochem. 279*, 151−163.
43. Stafford, W. F. (1994) Boundary analysis in sedimentation transport experiments: a procedure for obtaining sedimentation coefficient distributions using the time derivative of the concentration profile in *Modern Analytical Ultracentrifugation: Acquisition and Interpretation of Data for Biological and Synthetic Polymer systems* (Schuster, T. M. and Laue, T. M., Eds.) pp 119−137, Birkhauser, Boston.
44. Correia, J. J., Chacko, B. M., Lam, S. S., and Lin, K. (2001) Sedimentation studies reveal a direct role of phosphorylation in Smad3:Smad4 homo- and hetero-trimerization, *Biochemistry 40*, 1473−1482.
45. Stafford, W. F. (2000) Analysis of reversibly interacting macromolecular systems by time derivative sedimentation velocity, *Methods Enzymol. 323*, 303−325.
46. Schuck, P. (1998) Sedimentation analysis of noninteracting and self-associating solutes, using numerical solutions to the Lamm equation, *Biophys. J. 75*, 1503−1512.
47. Schuck, P. (2003) On the analysis of protein self-association by sedimentation velocity analytical ultracentrifugation, *Anal. Bioch. 320*, 104−124.
48. Tuganova, A., Boulantnikov, I., and Popov, K. M. (2002) Interaction between the individual isoenzymes of pyruvate dehydrogenase kinase and the inner lipoyl-bearing domain of transacetylase component of pyruvate dehydrogenase complex, *Biochem. J. 366*, 129−136.

49. Tuganova, A., and Popov, K. M. (2005) Role of protein-protein interactions in the regulation of pyruvate dehydrogenase kinase, *Biochem. J. 387*, 147−153.
50. Roche, T. E., Peng, T., Hu, L., Hiromasa, Y., Bao, H., and Gong, X. (2008) Roles of lipoyl domains in the function and regulation of the mammalian pyruvate dehydrogenase complex, in *Alpha Lipoic Acid: Energy Production, Antioxidant Activity and Health Effects* (Patel, M. S., and Packer, L., Eds.) pp 167−195, Taylor and Francis, Boca Raton, FL.
51. Brandt, D. R., Roche, T. E., and Pratt, M. L. (1983) Heterogeneity of binding sites for the pyruvate dehydrogenase component on the dihydrolipoyl transacetylase core of bovine kidney pyruvate dehydrogenase complex, *Biochemistry 22*, 2958−2965.
52. Tuganova, A., Klyuyeva, A., and Popov, K. M. (2007) Recognition of the inner lipoyl-bearing domain of dihydrolipoyl transacetylase and of the blood glucose-lowering compound AZD7545 by pyruvate dehydrogenase kinase 2, *Biochemistry 46*, 8592−8602.
53. Radke, G. A., Ono, K., Ravindran, S., and Roche, T. E. (1993) Critical role of a lipoyl cofactor of the dihydrolipoyl acetyltransferase in the binding and enhanced function of the pyruvate dehydrogenase kinase, *Biochem. Biophys. Res. Commun. 190*, 982−991.
54. Tso, S. C., Kato, M., Chuang, J. L., and Chuang, D. T. (2006) Structural determinants for cross-talk between pyruvate dehydrogenase kinase 3 and lipoyl domain 2 of the human pyruvate dehydrogenase complex, *J. Biol. Chem. 281*, 27197−27204.
55. Gyulai, L., Roth, Z., Leigh, J. S., and Chance, B. (1985) Bioenergetic studies of mitochondrial oxidative phosphorylation using ^{31}phosphorous NMR, *J. Biol. Chem. 260*, 3947−3954.
56. Hutson, S. M., Williams, G. D., Berkich, D. H., LaNoue, K. F., and Briggs, R. W. (1992) A ^{31}P NMR studty of mitochondrial inorganic phosphate visibility: effects of Ca^{2+}, Mn^{2+}, and pH gradient, *Biochemistry 31*, 1322−1330.
57. Joyal, J. L., and Aprille, J. R. (1992) The ATP-Mg/P_i carrier of rat liver mitochondria catalyzes a divalent electroneutral exchange, *J. Biol. Chem. 267*, 19198−19203.
58. Srere, P. A. (1981) Protein crystals as a model for mitochondrial matrix proteins, *Trends Biochem. Sci. 6*, 4−6.
59. Scalettar, B. A., Abney, J. R., and Hackenbrock, C. R. (1991) Dynamics, structure, and function are coupled in the mitochondrial matrix, *Proc. Natl. Acad. Sci. U.S.A. 88*, 8057−8061.
60. Zimmerman, S. B., and Minton, A. P. (1993) Macromolecular crowding: biochemical, biophysical, and physiological consequences, *Annu. Rev. Biophys. Biomol. Struct. 22*, 27−65.
61. Rohwer, J. M., Postma, P. W., Kholodenko, B. N., and Weserhoff, H. V. (1998) Implication of macromolecular crowding for signal transduction and metabolite channeling, *Proc. Natl. Acad. Sci. U.S.A. 95*, 10547−10552.
62. Dong, J. (2001) Expression, purification, and characterization of human pyruvate dehydrogenase kinase isoform 4, Ph.D. thesis, Kansas State University.
63. Korotchkina, L. G., and Patel, M. S. (2001) Site specificity of four pyruvate dehydrogenase kinase isozymes toward the three phosphorylation sites of human pyruvate dehydrogenase. *J. Biol. Chem. 279*, 37223−37229.
64. Pratt, M. L., and Roche, T. E. (1979) Mechanism of pyruvate inhibition of kidney pyruvate dehydrogenase kinase and synergistic inhibition by pyruvate and ADP, *J. Biol. Chem. 254*, 7191−7196.

BI7014772